ELSEVIER

Polymer 42 (2001) 6545–6556

polymer

www.elsevier.nl/locate/polymer

Reinforcement of poly(dimethylsiloxane) networks by mica flakes

Maged A. Osman[a], Ayman Atallah[a], Martin Müller[b], Ulrich W. Suter[a,*]

[a]*Department of Materials, Institute of Polymers, ETH Zentrum, CH-8092 Zurich, Switzerland*
[b]*Laboratory for Electronmicroscopy I, ETH Zentrum, CH-8092 Zurich, Switzerland*

Received 4 December 2000; received in revised form 5 February 2001; accepted 12 February 2001

Abstract

A poly(dimethylsiloxane) (PDMS) network was reinforced with spherical and plate-like particles. The shape, size distribution, aspect ratio, and surface area of the particles were examined by laser diffraction, gas adsorption, cation exchange, and scanning electron microscopy (SEM). The optimal ratio of cross-linker to PDMS precursor was ascertained from the mechanical properties of networks prepared with different cross-linker concentration. Homogeneous distribution of the filler in the polymer matrix as well as complete dispersion (disaggregation) of the particles are prerequisites for studying the influence of other parameters on the mechanical properties of composites. Mica platelets increased the elastic modulus of PDMS dramatically and were much superior to glass spheres with similar diameter. The modulus rose with increasing diameter and aspect ratio as well as with the volume fraction of the particles. The ultimate strength of the composite was also better enhanced by the plate-like particles than by spheres. However, the strength enhancement was less dramatic and the dependence on the particle size was reversed compared to that of the modulus. The tensile strength increased with increasing volume fraction of the filler but the rise was probably limited in the case of large particles by the emerging agglomeration at high loading. The ultimate elongation of the mica composites was comparable to that of glass spheres. The polymer chains did not intercalate the aluminosilicate layers of mica, as expected.

Keywords: Poly(dimethylsiloxane); PDMS; Network

1. Introduction

Polysiloxanes have been industrially exploited for a long time and nowadays they play an important role in different applications because of their high thermal stability, low surface tension and outstanding dielectric properties [1–3]. Their elastomeric networks also remain elastic over a wide range of temperature. Poly(dimethylsiloxane) (PDMS) is the most prevalent member of this class of materials, but its mechanical strength in the unfilled state is poor [3,4]. For this and other reasons, most applications require that PDMS be reinforced by particulate fillers [5–7]. The most widely used fillers in polysiloxanes are silica and carbon black, which are isometric, i.e. nearly spherical. However, acicular fillers, such as fibres, have also been applied. Composites of fibrous fillers usually show superior mechanical properties in the orientation direction of the fibres (orientation inevitably takes place during processing) but are weak in the others. Anisometric fillers, whose dimensions in two directions are significantly larger than in the third, i.e. platelets, were given much less attention, although they are expected to give superior two-dimensional reinforcement.

Better reinforcement is usually achieved by increasing the surface area of the filler, since the contact area, and consequently the interaction between the polymer and the filler, is increased. Enhanced interaction improves the wetting and adhesion of the polymer to the filler and larger contact area allows better transfer of the stress from the matrix to the filler. Therefore, fillers with small particle size, i.e. high surface area, are favoured in particulate reinforced polymers and nanocomposites are popular nowadays. However, the amount of nanoparticles which can be incorporated into a polymer matrix is limited by the huge increase in viscosity and the poor dispersability of small particles. Recently, Yuan and Mark [8] reported significant improvement of the mechanical properties of PDMS by blending it with isometric nano-sized fumed silica particles. Precipitation of the silica particles in situ also led to better dispersion of the filler and hence enhanced reinforcement [8,9].

Clay fillers such as smectites, e.g. montmorillonite, are plate-like particles which consist of negatively charged 1 nm thick aluminosilicate layers held together by interlayer cations. They are known to swell in water, so that they can

* Corresponding author. Tel.: +41-1-632-3127; fax: +41-1-632-1096.
E-mail address: suter@ifp.mat.ethz.ch (U.W. Suter).

0032-3861/01/$ - see front matter © 2001 Elsevier Science Ltd. All rights reserved.
PII: S0032-3861(01)00128-8

be easily delaminated to give nano-sized platelets with large specific surface area (SSA), whose surface cations can be exchanged with organic ammonium ions. Nanocomposites of such exfoliated organo-montmorillonites (OMT) with PDMS have been described by Burnside and Giannnelis [10,11]. Their results indicate that the elastic modulus of these composites can be three times that of the polymer matrix. Wang et. al. [12] intercalated PDMS in the galleries of OMT and showed that in this way a substantial increase in the tensile strength, comparable to that obtained with aerosilica nano-fillers, can be obtained. All of the aforementioned studies used hydroxyl-terminated precursors to build up the elastomeric network. Takeuchi and Cohen [13] studied the reinforcing effect of OMT on PDMS networks prepared from hydroxyl- or vinyl-terminated precursors. They observed a higher modulus only in defect networks prepared from hydroxyl-terminated precursors. No improvement in the modulus of networks synthesized from vinyl-terminated precursors could be obtained. They concluded that no reinforcement is achieved unless the polymer chains have hydroxyl end groups, which can be anchored to the silicate filler.

However, vinyl-terminated PDMS, which can be cross-linked by hydrosilylation to give elastomeric networks, is quite popular in the industry because of the ease and reliability of this reaction. Such networks are specially suited for high-voltage electric applications, where traces of moisture are critical. Muscovite mica is a 2:1 layered aluminosilicate (ideal formula $K_2Al_4(Al_2Si_6O_{20})(OH)_4$), which is of particular interest for electric insulation because of its outstanding corona resistance and insulation properties [14]. Each 2:1 layer consists of two tetrahedral silica sheets sandwiching an alumina octahedral sheet and is about 1 nm thick. Since on average one Si atom out of four in the tetrahedral sheets is replaced by Al, the layers are negatively charged. These charges are compensated by interlayer cations, mostly potassium, and the layers are held together in stacks by electrostatic and Van der Waals forces. In contrast to smectites, these stacks neither swell nor can they be delaminated under ambient conditions and represent the primary particles of ground mica. PDMS networks from vinyl-terminated precursors highly filled with muscovite are, therefore, of special interest for high-voltage insulation. Since the dielectric strength usually goes hand in hand with the mechanical strength, such composites are also needed for applications other than electric insulation. In other words, PDMS-mica composites are of interest from the electrical as well as from the mechanical point of view.

The reinforcement of thermoplasts by ground mica has been the subject of several studies [15–17] but still little is known about the correlation between composite properties and morphology of the filler particles. Also the influence of the granulimetric properties of plate-like particles on the mechanical properties of elastomeric networks has not been studied yet. Here, the reinforcing effect of mica flakes on a PDMS network obtained from a vinyl-terminated precursor is described and the mechanical properties of the composites are compared to those of PDMS filled with glass spheres of similar particle size.

2. Experimental

2.1. Materials

Vinyl-terminated PDMS (DMS-V31, $\eta_{25} = 1000$ cSt, 0.18–0.26% vinyl) and a platinum carbonyl complex (SIP 6829.0, 3–3.5% Pt) were purchased from Gelest Inc. (PA, USA). The number-average molecular weight M_n of DMS-V31, denoted by the supplier to be 28×10^3, was found by ^{1}H NMR (repetition rate = 35.5 s, 90° pulse, resolution = 0.1 Hz/point) to be $19 (\pm 1) \times 10^3$ assuming an average functionality of two. Poly(methylhydrosiloxane) (PMHS, $\eta_{25} = 15$–40 cSt, nominal $M_n = (1.7–3.2) \times 10^3$), whose M_n was found by ^{1}H NMR (same conditions as above) to be $2.2 (\pm 0.1) \times 10^3$, was purchased from Aldrich (Buchs, Switzerland). The NMR measurements of the precursors were taken to be an accurate measure of the molecular weight, since they correlate well with gel permeation chromatographic data [18].

Wet ground muscovite (mica R 180 and SX 400) was obtained from Microfine Minerals (Derby, UK), while the mica fines was a waste product of the mica-paper manufacture and was supplied by von Roll Isola (Breitenbach, Switzerland). Glass microspheres (Spheriglass 3000) were delivered by Potters–Ballotini (Düsseldorf, D). All fillers were washed with water and methanol, then dried before use to get rid of the processing auxiliaries often added during manufacture, which may interfere with the cross-linking reaction or affect the filler-matrix interaction.

2.2. Particle size

The particle size distribution (PSD) of the fillers was measured by a laser diffraction technique (Mastersizer X, Malvern Instruments, Malvern, UK) in dilute aqueous suspensions (sodium polyphosphate was added to help the dispersion). The suspensions were sonicated prior to the measurement in order to disperse (disintegrate) the agglomerates. The glass powder particles are isometric and their size measurement is straight forward, while the mica particles are platelets but their size distribution is given in equivalent spherical diameter d_v (diameter of a sphere, which has the same volume as that swept out by the rotating particle).

2.3. Surface area

2.3.1. Nitrogen adsorption (BET)

The SSA of the fillers was determined by the Brunauer–Emmett–Teller gas adsorption method using a Gemini III 2375 surface area analyzer (Micromeritics Instruments, Norcross, USA). Prior to the measurement, the samples were dried at 80°C under vacuum over night, then

scavenged with nitrogen on a FlowPrep 060 Degasser (Micromeritics) at 100°C for 2–3 h.

2.3.2. Cation exchange

The surface area of the mica particles dispersed in aqueous suspensions was determined by measuring their cation exchange capacity (CEC) using triethylenetetramine–Cu complex [19]. The $Cu(trien)^{2+}$ concentration was photometrically measured on a Cary 1E UV–vis spectrophotometer (Varian, Palo Alto, USA) at $\lambda_{max} = 255$. The surface area of the particle faces was calculated from the CEC values.

2.4. Sample preparation

2.4.1. Unfilled PDMS

The required amounts of DMS-V31 and catalyst (35 ppm Pt of the total sample weight) were thoroughly mixed before the corresponding amount of cross-linker (PMHS) was added. The well stirred mixture was then poured into a Teflon mould and degassed under reduced pressure before curing at 100°C for 3 h. The ca. 1 mm thick sheet so obtained was carefully released from the mould, while avoiding to scratch the surface. Careful releasing proved to be critical in the unfilled networks, since flaws lead to lower tensile strength. Dumbbell shaped samples were stamped out of these sheets with a stainless steel cutter.

2.4.2. Composites

The required amount of filler and DMS-V31 were carefully mixed and sonicated before the catalyst (40 ppm Pt of the total polymer weight) was added. After stirring 12.5 mol% PMHS into the mixture, it was degassed and poured in a Teflon mould. The paste was carefully homogenized in the mould with a spatula and degassed once more before curing at 100°C for 3 h. Pastes which were too viscous to give planar sheets on molding in this way (14% load) were pressed and cured in a brass frame between two Teflon plates under reduced pressure. Dumbbell shaped samples were stamped out of the resulting ca. 1 mm thick sheet with a stainless steel cutter.

2.5. Mechanical measurements

Stress–strain measurements of dumbbell-shaped specimens ($2 \times 0.6 \times 0.1$ cm^3 test region) in uniaxial extension were carried out on a Mecmesin M1000 E tensile testing machine (West Sussex, UK) at small extension ($\leq$6%). All measurements were taken at room temperature and the average of four measurements for each sample is reported. The undeformed cross-sectional area A^* was determined by measuring the thickness and width of each sample with a micrometer. The reduced stress (elastic modulus) was calculated from

$$[f^*] = f^*/(\alpha - \alpha^{-2}),$$

where $\alpha = L/L_0$ is the elongation, and f^* is the nominal stress given by $f^* = f/A^*$ with f the measured force.

2.6. X-ray diffraction (XRD)

Wide-angle diffraction patterns (WAXRD) from the mica powder as well as from the 10 vol% composites were collected at room temperature on a Philips PW 1820-APD 1700 diffractometer using monochromatized CuKα ($\lambda = 0.15419$ nm) radiation (40 mA, 30 kV). The instrument was equipped with a graphite monochromator and a proportional xenon detector.

2.7. Scanning electron microscopy

Cross-sections were cut perpendicular and parallel to the horizontal plane of the samples using a razor blade. The faces of the sections were sputter coated with 5 nm of Pt and observed in a Hitachi S-900 'in-lens' field emission scanning electron microscope (FESEM) at 20 kV.

2.8. Thermogravimetric analysis

The thermogravimetric analysis (TGA) was carried out in an air stream as well as under flowing nitrogen at a heating rate of 20°C/min on a Perkin–Elmer 7 thermal analysis system (Perkin–Elmer, Norwalk, CT). The gas flow in both cases was ca. 50 ml/min.

3. Results and discussion

3.1. Filler characterization

Although it is well recognized that the morphology of the particulate filler strongly influences the performance of a composite, very often the filler characterization is not given the necessary attention. This is probably due to the complexity of powder characterization and the lack of unequivocal measuring techniques for ground particles (non-spherical with broad size distribution) [20–22]. Among the most important filler characteristics, which determine the performance of a composite, are the shape, aspect ratio, surface area, PSD and tendency to agglomeration. In this study, the fillers were characterized by determining their PSD (laser diffraction) and surface area (gas adsorption and cation exchange) as well as by microscopic (SEM) observation. The measured data for the mica and glass powder used in this investigation are given in Table 1.

The SEM micrograph of the glass powder (Fig. 1a) shows that the primary particles are spheres with a broad size distribution and confirms the particle size measured by laser diffraction. The particle diameter ($d_{BET} = 10.1$ μ) calculated from the SSA measurement [23] also correlates well with these data showing that the surface of Spheriglass is not porous and that the particles are well dispersed in the liquid. The mica particles (Fig. 1b–d) are platelets of different shapes, sizes and elongation (length to width)

Table 1
Filler particle properties (SSA, specific surface area; SSA_V, surface area per volume unit; $d_{V0.5}$, median volume diameter; $d_{S0.5}$, median area diameter; CEC, cation exchange capacity; SFA, specific face area (two faces); SFA_v, specific face area per unit volume; t_{av}, average particle thickness; Aspect ratio, $d_{S0.5}/t_{av}$)

Filler type	BET		Laser diffraction		Cation exchange				
	SSA (m^2/g)	SSA_V (m^2/ml)	$d_{V0.5}$ (μm)	$d_{S0.5}$ (μm)	CEC (μmol/g)	SFA (m^2/g)	SFA_V (m^2/ml)	t_{av} (μm)	Aspect ratio
Spheriglass	0.2	0.6	22.3	6.3					1
Mica SX 400	6.0	16.1	12.4	8.0	13.69	3.9	10.4	0.192	42
Mica R 180	6.2	17.2	50.9	23.0	10.39	2.9	8.2	0.243	94
Mica fines	2.3	6.0	85.3	41.0	7.77	2.2	5.8	0.344	119

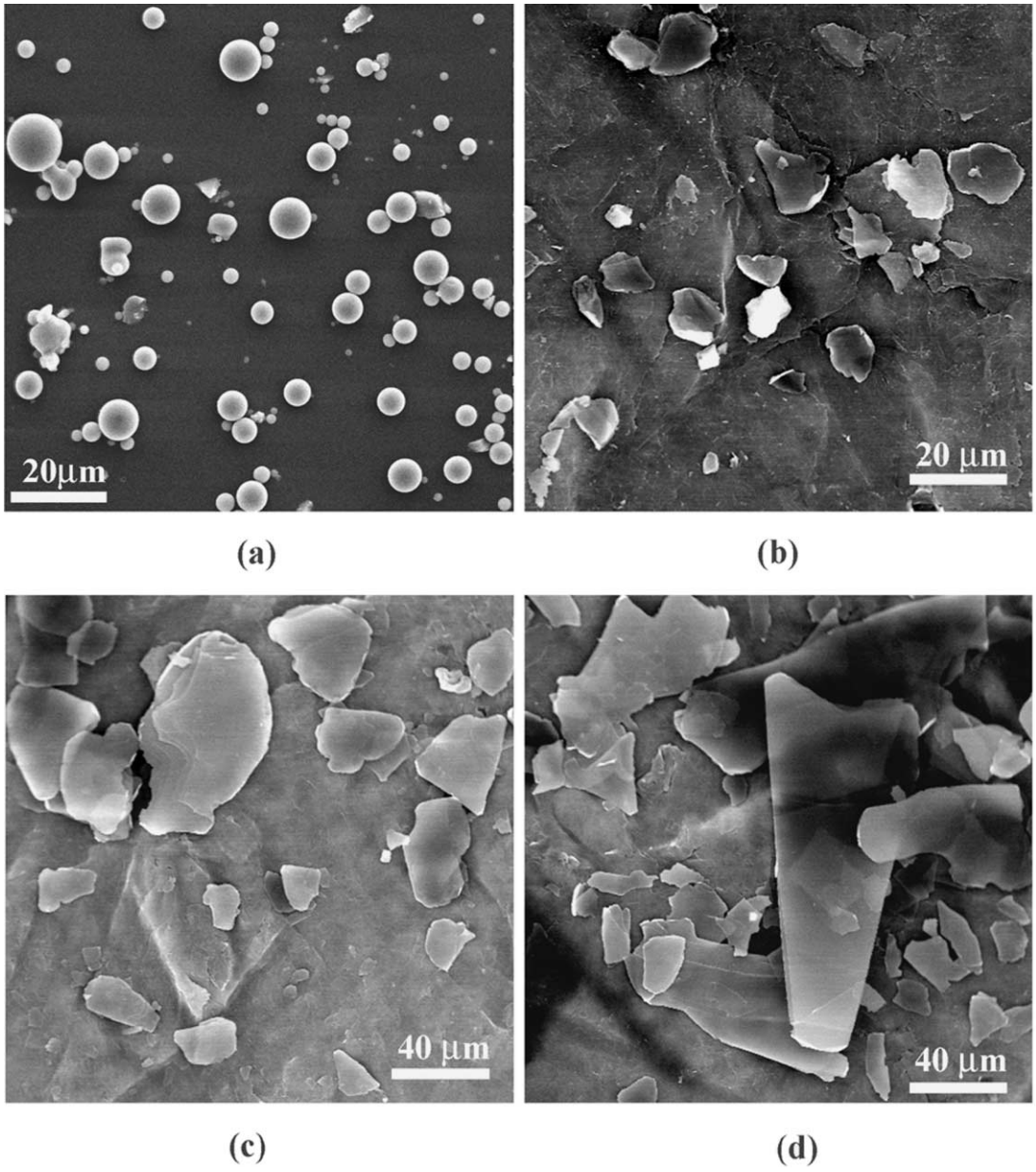

Fig. 1. SEM micrographs of the fillers: (a) Spheriglass 3000 CP00, (b) mica SX 400, (c) mica R 180, and (d) mica fines.

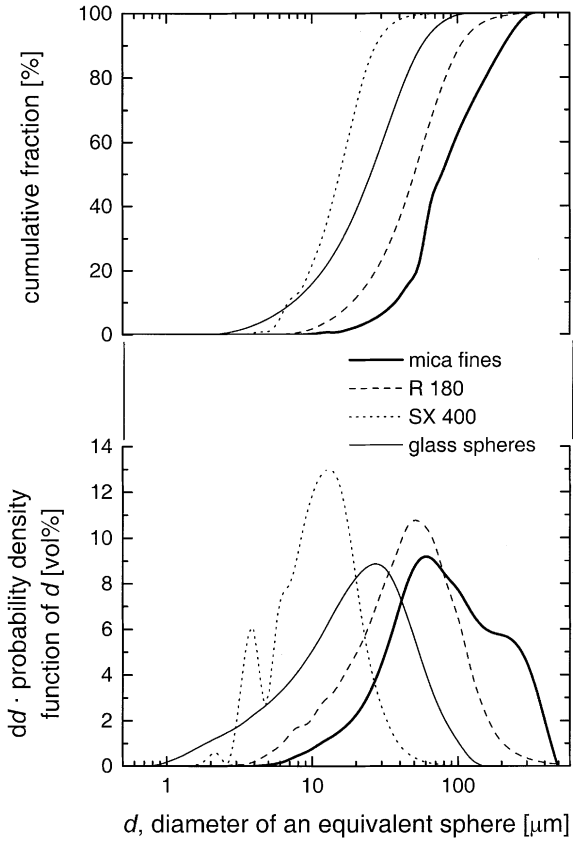

Fig. 2. Particle size distribution of the fillers.

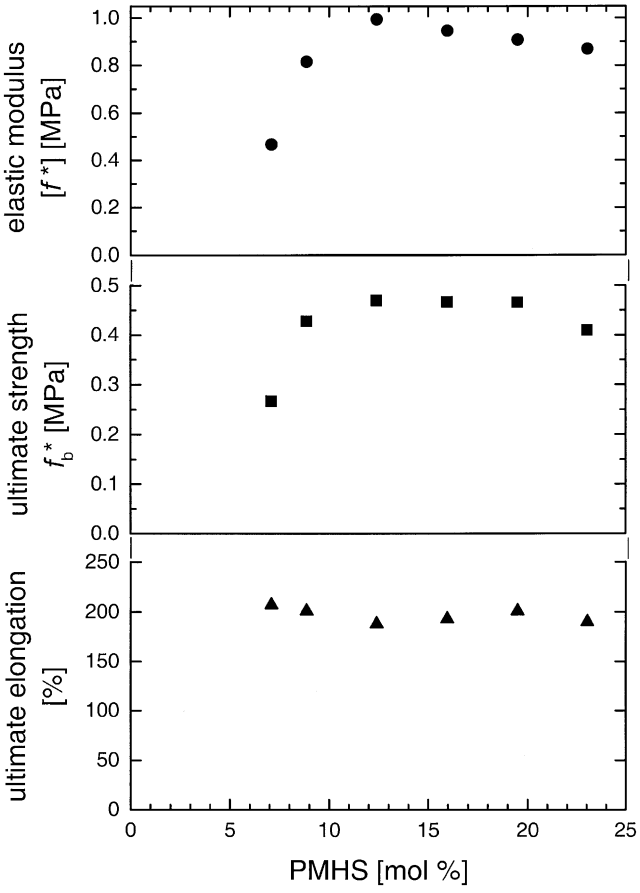

Fig. 3. Dependence of the mechanical properties of the unfilled PDMS network on the amount of cross-linker in mol% of the vinyl-terminated precursor.

ratio, i.e. the primary particles are longer than wide with irregular outlines and their minor axis is the thickness (t). Like all crystalline fine particles, they tend to agglomerate to reduce the total surface energy. They agglomerate mainly face-to-face but edge-to-face agglomeration can also take place. Their tendency to agglomerate is enhanced by the large flat faces of the platelets as well as by the adhesion forces arising from their chemical structure. Therefore, they have to be carefully dispersed before every measurement. Their particle size analysis is also hampered by their geometry, since most analytical methods assume a spherical shape, which renders the data interpretation for anisometric particles more difficult [24]. For plate-like particles, it becomes necessary to find a form factor or an aspect ratio (major to minor axis). However, accurate measurement of the particle thickness is quite difficult, especially for thin particles with broad distribution (an adequate number of representative non-agglomerated particles have to be considered). Assuming a cylindrical disc model, Baudet et al. developed a method for estimating the average aspect ratio of plate-like particles by laser diffraction, which uses isodiametric particles to calibrate the projected area [25]. Based on this work, Ward-Smith and Wedd [26] calculated the median area diameter ($d_{S0.5}$) of such particles from laser diffraction measurements using the Mie theory by comparing the actual particle volume concentration with that measured. The median volume ($d_{V0.5}$) and area ($d_{S0.5}$) diameters of the mica particles were estimated by this method and are given in Table 1. The PSD measurements (Fig. 2) also showed a relatively broad log-normal distribution, which is typical for ground powders.

The SSA of the fillers was measured by the gas adsorption method (Table 1). However, the values obtained for some of the powders are probably too high due to gas entrapments. Although the mica surface is not porous, nitrogen can be retained in the pores between the primary particles within the aggregates and agglomerates as well as in the lateral openings of the interlayer galleries [27]. The surface area of mica can be more precisely determined by measuring its CEC, since only the surface cations are exchangeable at ambient conditions and the area per charge (0.47 nm^2) is known [28]. However, this method does only give the specific face area (SFA) and not the total SSA, since the edges of the mica particles do not carry cations but anions [27]. Approximating the mica particle shape to a cylindrical disc, the average thickness (t_{av}) can be calculated from SFA and the aspect ratio can then be estimated from $d_{S0.5}$ and t_{av}. These data are presented in Table 1 as well as the surface and face area per unit volume SSA_V and SFA_V, which are more relevant for composites, since they take

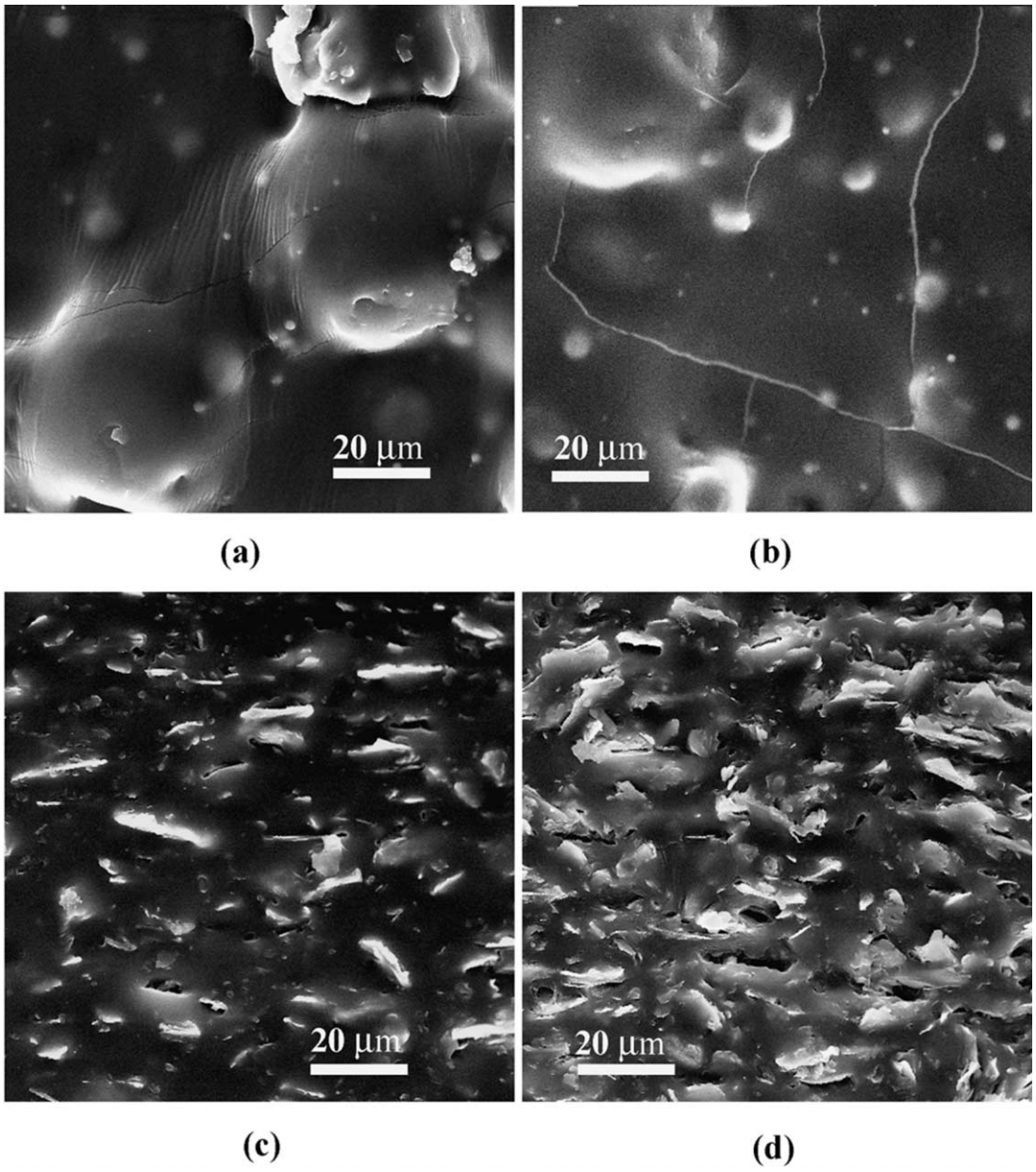

Fig. 4. SEM micrographs of sections cut perpendicular to the horizontal plane of composite samples: (a) 10 vol% spheriglass, (b) 14 vol% Spheriglass, (c) 10 vol% mica SX 400, and (d) 14 vol% mica SX 400.

care of the differences in density of the materials involved and represent the contact area between the filler and the matrix. In this context, it should be remarked that the thickness of lamellar particles becomes automatically smaller during milling due to partial delamination, i.e. small particles are on average thinner than the large ones. Therefore, the lateral surface area of the mica particles is expected to be smaller than 5% of their face area. The data given in Table 1 are characteristic for the primary particles of the fillers in water and the polymer matrix as long as they are completely dispersed.

3.2. Mechanical properties

Model PDMS networks are usually prepared by end-linking a difunctional (e.g. vinyl-terminated) PDMS with a tri- or tetrafunctional cross-linker, e.g. tetrakis(dimethylsiloxy)silane. In absence of side reactions, the ratio (r) of silane hydrogens to vinyl groups is approximately unity [18,29]. The optimal ratio of cross-linker to vinyl groups (r_{opt}) is that which gives a network with the lowest amount of dangling chains, that is the lowest degree of equilibrium swelling, and leads to the highest elastic modulus [18,29–31]. In real networks, r_{opt} is often larger than unity due to

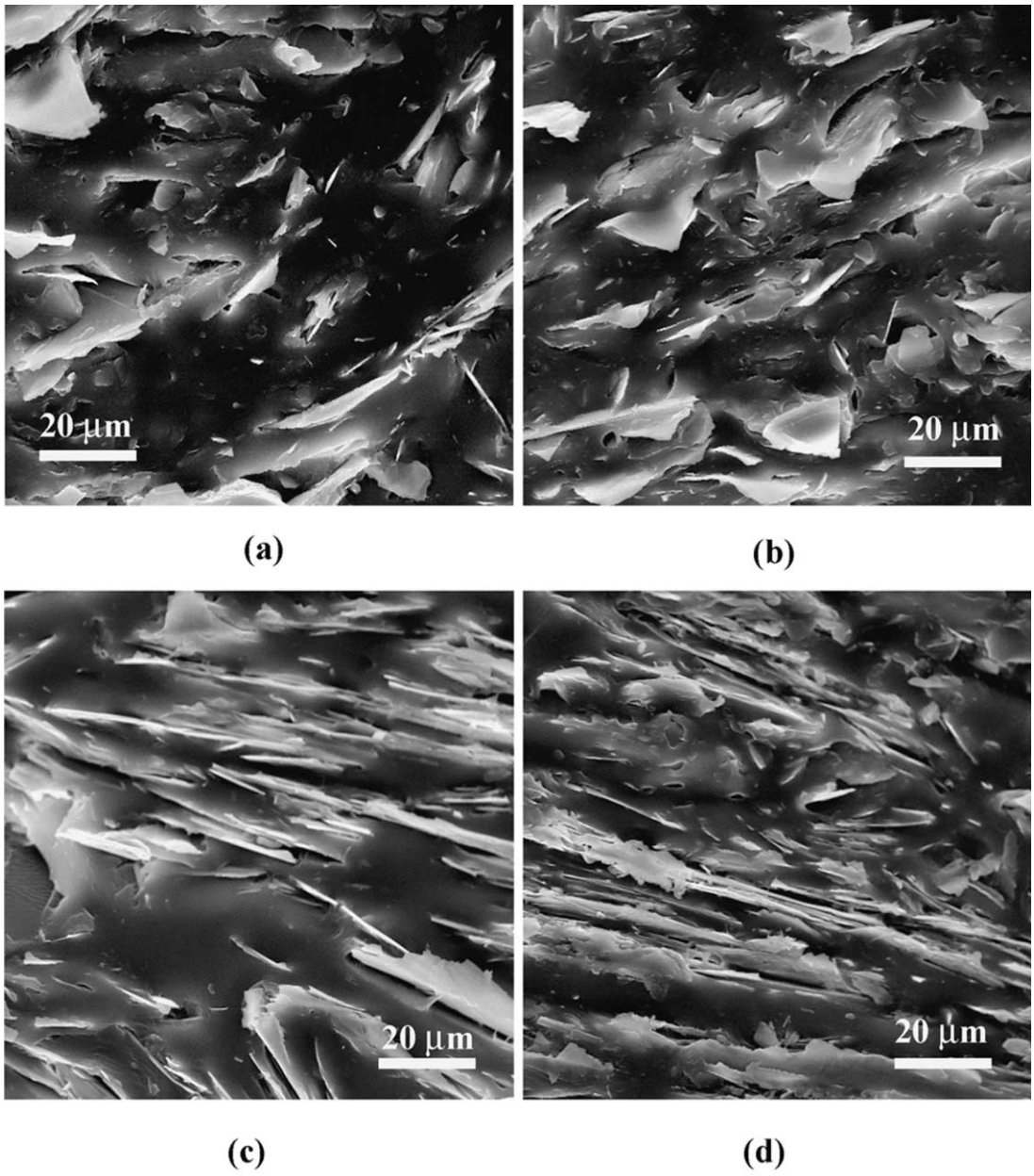

Fig. 5. SEM micrographs of sections cut perpendicular to the horizontal plane of composite samples: (a) 10 vol% mica R 180, (b) 14 vol% mica R 180, (c) 10 vol% mica fines, and (d) 14 vol% mica fines.

side reactions, kinetic (viscosity) or steric effects, and this ratio has to be experimentally determined [30,31]. In this study, a multifunctional cross-linker (PMHS) was used because of its popularity in the industry and r_{opt} was determined by measuring the mechanical properties of networks prepared with different r. This approach was preferred to the often used equilibrium swelling measurement, since it is directly linked to the goal of this study (reinforcement of PDMS networks). Fig. 3 shows the dependence of the elastic reduced stress $[f^*]$ and the tensile strength f_b^* of the PDMS network on r. It can be easily seen that there is an optimal concentration of cross-linker (in the vicinity of 12.5 mol%), above which the mechanical properties of the network deteriorate. A cross-linker concentration of 12.5 mol% was consequently used to prepare the composites. Contrary to modulus and strength, the ultimate elongation (elongation to break) does not significantly depend on the amount of cross-linker (Fig. 3).

The properties of particulate-filled composites are generally determined by the component properties, composition, structure (distribution), particle–particle interaction (agglomeration) and particle-matrix interaction (wetting and adhesion). The extent to which particles agglomerate depends on the balance between the attractive

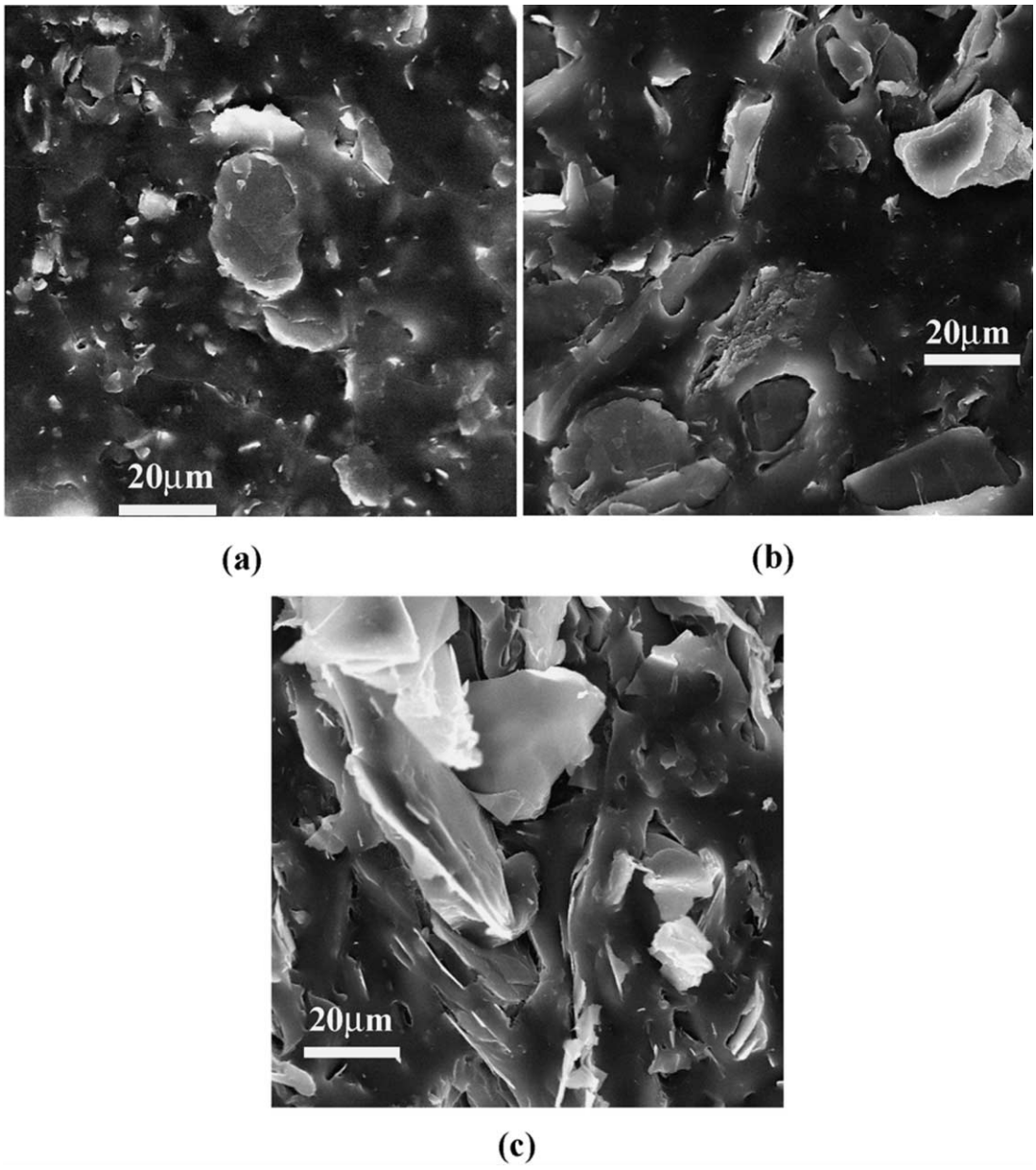

Fig. 6. SEM micrographs of sections cut parallel to the horizontal plane of composite samples: (a) 10 vol% SX 400, (b) 10 vol% mica R 180, and (c) 10 vol% mica fines.

and repulsive forces among the particles and between them and the matrix as well as on the processing conditions (shear forces). The morphology of the composites is also often considered to be of crucial importance for the mechanical properties: therefore, the prepared composites were examined by scanning electron microscopy (SEM). The SEM micrographs of sections cut perpendicular to the horizontal plane (parallel to the sheet's flat surface) of the composite samples (Figs. 4 and 5) show that the filler is uniformly distributed in the PDMS matrix even at the highest loading. Optically, no sign of agglomeration can be observed in all micrographs except in the 14 vol% mica fines composite (Fig. 5d). The picture indicates that this probably is not a simple geometric packing effect and the attraction between the platelets seem to increase with increasing face area and decreasing interparticle distance, so that the mica fines particles tend to agglomerate above 10 vol%. The micrographs of the parallel and perpendicular sections (Figs. 4–6) also show that the platelets are randomly oriented with a slight tendency to lie parallel to the horizontal plane of the sample.

The influence of increasing volume fraction of the different fillers on $[f^*]$ of the composites is shown in Fig. 7. It can be seen that the modulus increases with increasing volume fraction for all fillers and that the reinforcing effect of the glass spheres is very small compared to

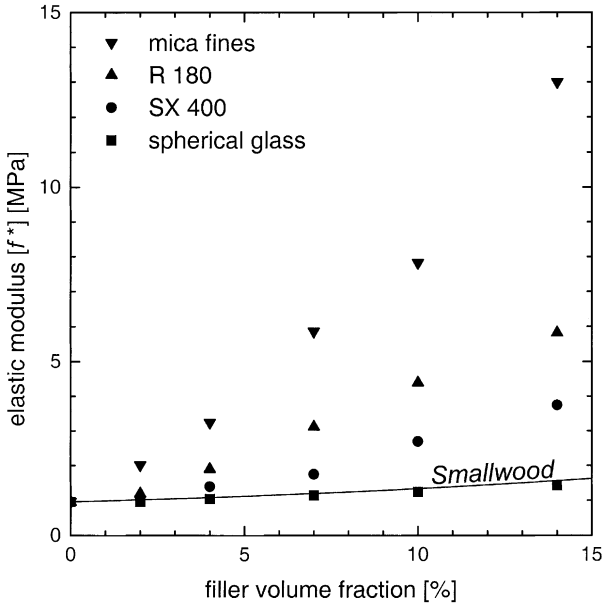

Fig. 7. The elastic modulus in function of the filler volume fraction for the random composites. The line represents the theory by Smallwood ($E/E_0 = 1 + 2.5\varphi + 14.1\varphi^2$, for random composites with spheres [32]).

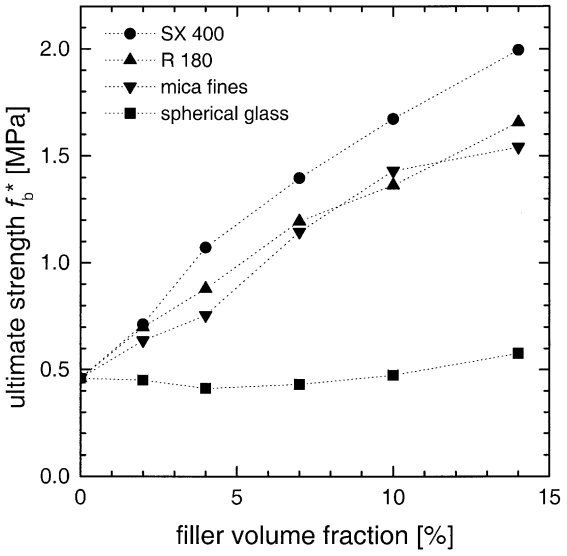

Fig. 9. Comparison of the reinforcing effect of fillers with different shape and size, and the dependence of the ultimate strength of the composites on the filler volume fraction.

that of the mica platelets. At all filler concentrations, the reinforcing effect increases dramatically with increasing aspect ratio of the particles (Fig. 8), so that $[f^*]$ of the mica fines composite at a loading of 14 vol% is 13 times higher than that of the polymer matrix. Even the R 180 particles, which has a smaller aspect ratio, increases $[f^*]$ sixfold at the same filler volume fraction. This increase in modulus is much higher than that reported for PDMS nanocomposites obtained from hydroxyl-terminated precursors and exfoliated OMT (threefold) [11]. Fig. 7 also shows that $[f^*]$ does not reach a saturation value, i.e. up to 14 vol% no plateau value is reached and further increase can be expected for higher loading. This is in contrast to the results obtained with OMT nanocomposites, where a maximum relative modulus was reached at 4% loading [11]. It should be noted that the particle agglomeration in the 14 vol% mica fines composite did not limit the increase in elastic modulus. It is often stated in the literature that the reinforcing effect of particulates increases with decreasing diameter. This may be true within isometric particles, where the decrease in diameter is accompanied by an increase in surface (contact) area, but not within particles of different shapes. Fig. 7 shows that the reinforcing effect of mica SX 400, which is similar to Spheriglass 3000 in diameter, is much higher than that of the spheres.

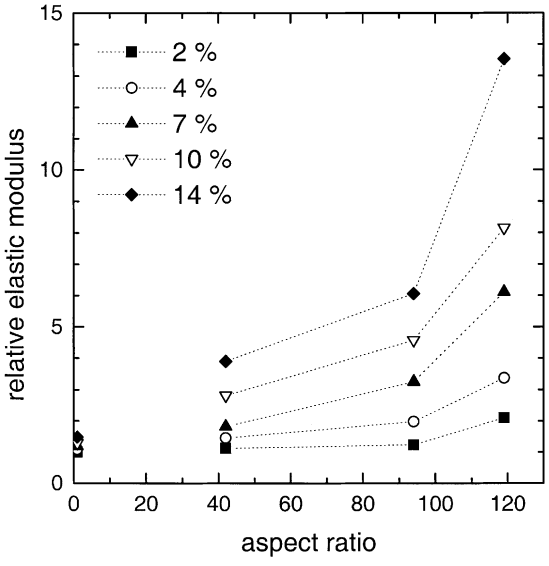

Fig. 8. Dependence of the relative elastic modulus on the aspect ratio of the filler particles.

The dependence of the composites, ultimate strength on the filler type and volume fraction is shown in Fig. 9. Again the glass spheres had minimal effect compared to the mica platelets and SX 400 increased f_b^* by a factor of 4.5 at 14 vol%. However, the differences in reinforcement obtained with the different-sized platelets were relatively small and the order of enhancement with respect to the particle size is reversed compared to that seen in the modulus. In other words, the SX 400 platelets with the smallest diameter led to the highest f_b^* values. No saturation value in tensile strength was reached up to a loading of 14 vol% in all cases except with the mica fines, where the influence of the filler seem to level off at high loading, thus showing that the increase in f_b^* is limited by the agglomeration of the mica fines particles at 14 vol% loading. The dependence of the relative ultimate strength on the aspect ratio of the filler particles is shown in Fig. 10. At all filler concentrations, the tensile strength of the mica composites decreased with increasing particle aspect ratio but was always higher than that of the glass spheres. Whether the

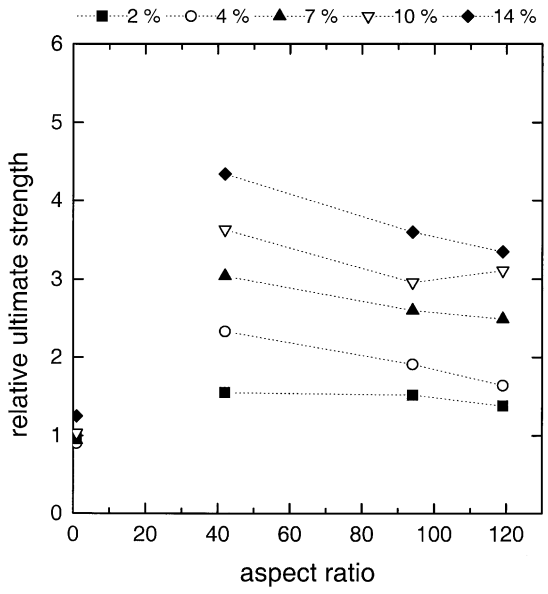

Fig. 10. Dependence of the relative ultimate strength on the aspect ratio of the filler particles.

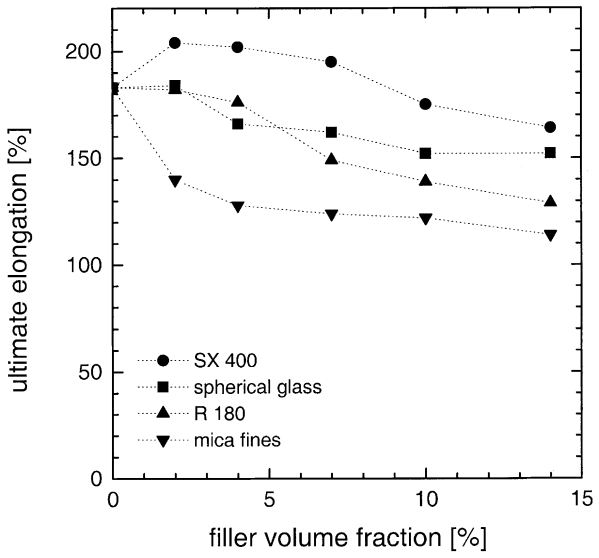

Fig. 11. Influence of the filler volume fraction on the ultimate elongation of PDMS composites.

decrease in f_b^* is a sign of optically not detected particle agglomeration remains to be investigated. The large increase in modulus and strength of the mica-PDMS composites obtained from vinyl-terminated precursors reported here is in contrast to the results of Takeuchi and Cohen for OMT composites [13].

The effect of the filler type and volume fraction on the ultimate elongation (elongation at break, α_b) of the composites is shown in Fig. 11. At high loading, α_b decreased irrespective of the shape and size of the particles. The mica fines had the strongest effect, while the SX 400 decreased α_b only slightly. However, the correlation between α_b and the filler volume fraction was not always linear and at low loading SX 400 even increased the ultimate elongation before decreasing it. A similar observation was made by Wang et al. [12] for the OMT nanocomposites. In contrast, the mica fines decreased α_b strongly at low loading, then the influence leveled off.

From these results it seems that the elastic modulus depends strongly on the distribution of the particulates (agglomerates or primary particles) in the polymer matrix, while the ultimate strength enhancement is limited by the particle agglomeration. [f^*] increases with increasing filler volume fraction as long as a homogeneous structure is ensured, but a plateau value is reached when the particles are inhomogenously distributed. The stress (and the resulting strain) used to determine the modulus is too small to separate agglomerated particles and therefore, the modulus enhancement is not significantly affected by the particle agglomeration. In other words, even agglomerated particles can lead to an increase in modulus if they are uniformly distributed in the matrix. On the other hand, if the filler is not well dispersed and the force used to determine f_b^* is higher than that necessary to take the agglomerates apart (which may be the case during the strength measurement), a crack is initiated and this limits the tensile strength.

3.3. X-ray diffraction

The WAXRD patterns of the mica fines particles as well as those of the 10 vol% mica-PDMS composites are plotted

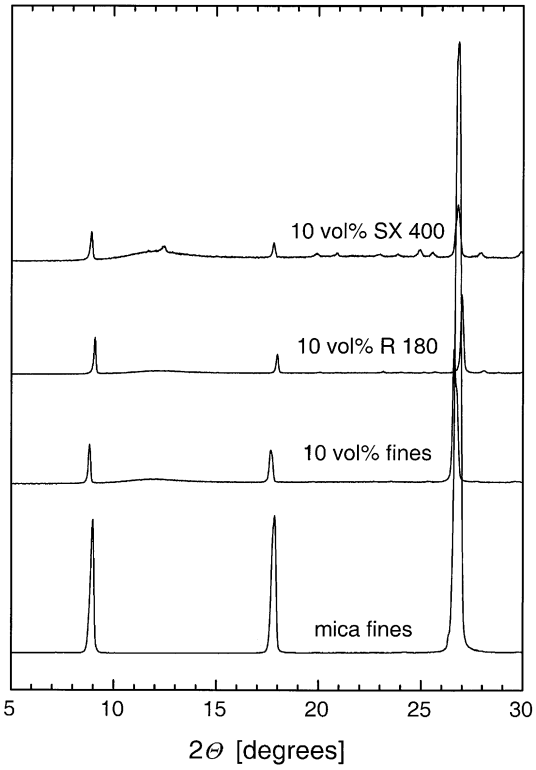

Fig. 12. Comparison of the WXRD patterns of muscovite platelets with those of the 10 vol% mica-PDMS composites.

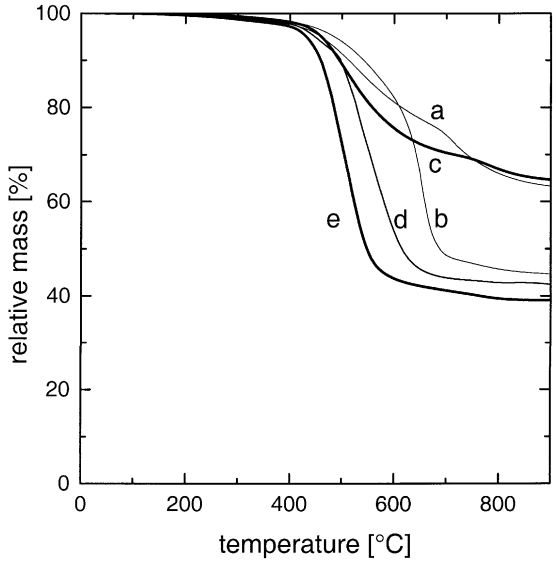

Fig. 13. TGA traces recorded under nitrogen: (a) unfilled PDMS, (b) 10 vol% Spheriglass composite, (c) 10 vol% SX 400 composite, (d) 10 vol% mica R 180 composite, and (e) 10 vol% mica fines composite.

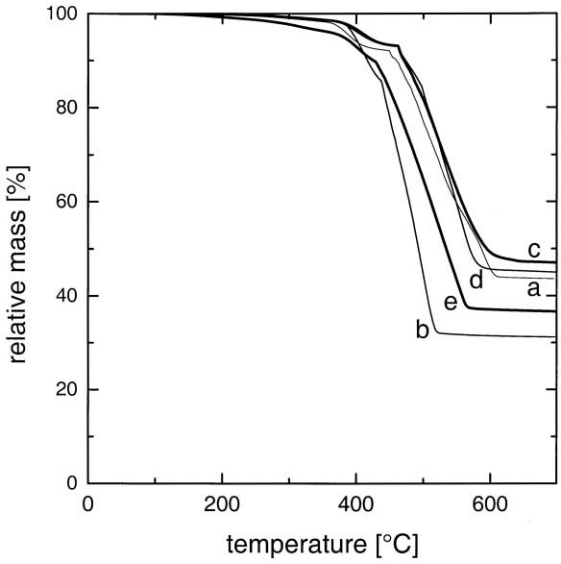

Fig. 14. TGA traces recorded under air: (a) unfilled PDMS, (b) 10 vol% Spheriglass composite, (c) 10 vol% SX 400 composite, (d) 10 vol% mica R 180 composite, and (e) 10 vol% mica fines composite.

in Fig. 12, showing the 001, 002 and 003 reflections. As can be seen, there is neither a shift nor a broadening of the peaks, indicating that the polymer chains did not intercalate the aluminosilicate layers, as expected.

3.4. Thermal stability

The weight loss of the 10 vol% composites with increasing temperature in a nitrogen atmosphere is plotted in Fig. 13. In contrast to the organo-modified aluminosilicates [10,12], the untreated glass particles as well as the mica fines and R 180 enhanced the thermal degradation of PDMS, while SX 400 did not, which indicates that this enhancement is due to a catalytic effect. The oxidative degradation of the same composites is shown in Fig.14. It can be seen that only the mica fines and the glass particles enhanced the oxidation of PDMS, thus supporting the catalysis hypothesis. The catalytic effect probably depends on the chemical composition and the nature of the surface cations of the particles, which in turn depends on the origin of the mineral.

4. Conclusions

The elastic modulus of PDMS networks is dramatically increased by the incorporation of plate-like particles. The modulus enhancement depends on the aspect ratio and volume fraction of the particles (agglomerates or primary particles), in a manner similar to that implied by the empirical Halpin–Tsai equation, as well as on their distribution in the matrix. In contrast, the ultimate strength of the composite is more enhanced by small platelets and strongly depends on the dispersion of the filler. The composite strength is also proportional to the filler-volume-fraction but the increase in strength is limited by particle agglomeration, which emerges at high loading. It is quite important to ensure complete dispersion (disaggregation) and homogeneous distribution of the particulates in the polymer matrix before studying the influence of other parameters on the mechanical properties of composites.

Acknowledgements

We gratefully acknowledge financial support from the Swiss Commission for Technology and Innovation (CTI).

References

[1] Clarson SJ, Semlyen JA. Siloxane polymers. Englewood Cliffs, NJ: Prentice-Hall, 1993.
[2] Mark JE, Allcock HR, West R. Inorganic polymers. Englewood Cliffs, NJ: Prentice-Hall, 1992.
[3] Noll W. The chemistry and technology of silicones. New York: Academic Press, 1968.
[4] Erman B, Mark JE. Structures and properties of rubber-like networks. New York: Oxford University Press, 1997.
[5] Wagner MP. Rubber Chem Technol 1976;49:703.
[6] Boonstra BB. Polymer 1979;20:691.
[7] Voet A. J Polym Sci Macromol Rev 1980;15:327.
[8] Yuan QW, Mark JE. Macromol Chem Phys 1999;200:206.
[9] Wen J, Mark JE. Rubber Chem Technol 1995;67:806.
[10] Burnside SD, Giannelis EP. Chem Mater 1995;7:1597.
[11] Burnside SD, Giannelis EP. J Polym Sci Part B Polym Phys 2000;38:1595.
[12] Wang SJ, Long CF, Wang XY, Li Q, Qi ZN. J Appl Polym Sci 1998;69:1557.
[13] Takeuchi H, Cohen C. Macromolecules 1999;32:6792.
[14] Schüller KH, Brinkmann C. Ullmanns Encyklopädie der technischen Chemie, vol. 13. Weinheim/New York: Verlag Chemie, 1977. p. 359.

[15] Trotignon JP, Sanschagrin B, Piperaud M, Verdu J. Polym Compos 1982;3:230.
[16] Mitsuishi K, Kodama S, Kawasaki H. J Macromol Sci Phys 1987;B26:479.
[17] Malik TM, Faroqi MI, Vachet C. Polym Compos 1992;13:174.
[18] Venkataraman SK, Coyne L, Chambon F, Gottlieb M, Winter HH. Polymer 1989;30:2222.
[19] Osman MA, Suter UW. J Colloid Interface Sci 2000;224:112.
[20] Allen T. Particle size measurement. London: Chapman & Hall, 1997.
[21] Kissa E. Dispersions characterization, testing, and measurement. New York: Marcel Dekker, 1999.
[22] Xu R. Particle characterization: light scattering methods. Dordrecht: Kluwer Academic Publishers, 2000.
[23] German RM, Int J. Powder Metall 1996;32:365.
[24] Bowen P, Humphry-Baker R, Herard C. World Cong Part Technol 1998;3:270.
[25] Baudet G, Bizi M, Rona JP. Part Sci Technol 1993;11:73.
[26] Ward-Smith RS, Wedd MW. Malvern Internal Report.
[27] Jasmund K, Lagaly G. Tonminerale und Tone. Darmstadt: Steinkopff-Verlag, 1993.
[28] Osman MA, Suter UW. J Colloid Interface Sci 1999;214:400.
[29] Macosko CW, Benjamin GS. Pure Appl Chem 1981;53:1505.
[30] Macosko CW, Saam JC. Polym Bull 1987;18:463.
[31] Patel SK, Malone S, Cohen C, Gillmor JR, Colby RH. Macromolecules 1992;25:5241.
[32] Smallwood HM. J Appl Phys 1944;15:758.